



# Novel inhibitors of phosphorylation independent activity of GRK2 modulate cAMP signaling

Emiliana Echeverría<sup>1,2</sup> | Sonia Ripoll<sup>1,2</sup> | Lucas Fabián<sup>3</sup> | Carina Shayo<sup>4</sup> |  
Federico Monczor<sup>1,2</sup>  | Natalia C. Fernández<sup>1,2</sup> 

<sup>1</sup>Facultad de Farmacia y Bioquímica, Universidad de Buenos Aires, Buenos Aires, Argentina

<sup>2</sup>Instituto de Investigaciones Farmacológicas (ININFA-UBA-CONICET), Facultad de Farmacia y Bioquímica, Universidad de Buenos Aires, Buenos Aires, Argentina

<sup>3</sup>Instituto de Química y Metabolismo del Fármaco (IQUIMEFA-UBA-CONICET), Facultad de Farmacia y Bioquímica, Universidad de Buenos Aires, Buenos Aires, Argentina

<sup>4</sup>Laboratorio de Patología y Farmacología Molecular, Instituto de Biología y Medicina Experimental (IByME), CONICET, Buenos Aires, Argentina

## Correspondence

Natalia C. Fernández, Facultad de Farmacia y Bioquímica, Universidad de Buenos Aires, Buenos Aires, Argentina. Email: nfernandez@docente.ffyb.uba.ar

## Funding information

Fondo para la Investigación Científica y Tecnológica, Grant/Award Number: PICT 2015-2443 and PICT 2019-2586; Universidad de Buenos Aires, Grant/Award Number: UBACYT 2018 20020170200166BA01

## Abstract

G protein-coupled receptors kinase 2 (GRK2) plays a major role in receptor regulation and, as a consequence, in cell biology and physiology. GRK2-mediated receptor desensitization is performed by its kinase domain, which exerts receptor phosphorylation promoting G protein uncoupling and the cessation of signaling, and by its RGS homology (RH) domain, able to interrupt G protein signaling. Since GRK2 activity is exacerbated in several pathologies, many efforts to develop inhibitors have been conducted. Most of them were directed toward GRK2 kinase activity and showed encouraging results on *in vitro* systems and animal models. Nevertheless, limitations including unspecific effects or pharmacokinetics issues prevented them from advancing to clinical trials. Surprisingly, even though the RH domain demonstrated the ability to desensitize GPCRs, this domain has been less explored. Herein, we show *in vitro* activity of a series of compounds that, by inhibiting GRK2 RH domain, increase receptor cAMP response, avoid GRK2 translocation to the plasma membrane, inhibit coimmunoprecipitation of GRK2 with G $\alpha$ s subunit of heterotrimeric G protein, and prevent receptor desensitization. Also, we preliminarily evaluated candidates' ADMET properties and observed suitable lipophilicity and cytotoxicity. These novel inhibitors of phosphorylation-independent actions of GRK2 might be useful in elucidating other RH domain roles and lay the foundation for the development of innovative pharmacologic therapy for diseases where GRK2 activity is exacerbated.

## KEYWORDS

CADD, desensitization, GPCR, GRK2, RGS

**Abbreviations:** Amtha, amthamine; GPCR, G protein-coupled receptor; GRK2, G protein-coupled receptors kinase 2; H2R, histamine H2 receptor; RGS, regulator of GTPase activity; RH domain, RGS homology domain.

This is an open access article under the terms of the Creative Commons Attribution-NonCommercial-NoDerivs License, which permits use and distribution in any medium, provided the original work is properly cited, the use is non-commercial and no modifications or adaptations are made.

© 2022 The Authors. *Pharmacology Research & Perspectives* published by John Wiley & Sons Ltd, British Pharmacological Society and American Society for Pharmacology and Experimental Therapeutics.

## 1 | INTRODUCTION

Signal transduction is responsible for the coordinated function of every cell and organ within an organism. G protein-coupled receptors (GPCRs) represent the largest family of membrane proteins involved in cell signaling. They possess seven transmembrane domains and are associated with a heterotrimeric G protein to translate chemical and physical external signals into intracellular second messengers such as cAMP, diacylglycerol, inositol triphosphate (IP3), cGMP, and calcium.<sup>1</sup> These systems control key physiological functions, and their dysfunction contributes to several of the predominant human diseases. Accordingly, GPCRs represent the direct or indirect target of 35% of the therapeutic agents currently used.<sup>2</sup> Given the importance of these receptors as etiological agents of a variety of diseases, accessory proteins belonging to their signaling pathways are also considered potential therapeutic targets. GPCRs kinase type 2 (GRK2) mediates the desensitization of GPCRs, an adaptive process aimed at cutting off receptor signaling avoiding overstimulation that can be deleterious to cell survival.

GRK2 is a multidomain protein. According to the canonical model of GPCRs' desensitization, the kinase domain of GRK2 phosphorylates active receptors, which undergo rapid uncoupling from the heterotrimeric G protein, becoming unable to signal through it. GRK2 has been shown to phosphorylate a wide variety of GPCRs, including  $\alpha$  and  $\beta$ -adrenergic, angiotensin, endothelin, and histamine receptors among others. Reports show that GRK2 is also capable of regulating receptor signaling through mechanisms dependent on the GRK2 RH domain or homologous to RGS (regulator of G protein signaling) but independent of GPCRs phosphorylation. The RH domain is present at the N-terminal of GRK2 and is capable of binding directly to the G protein, causing its inactivation and preventing subsequent signaling.<sup>3-6</sup> Desensitization of GPCRs signaling in a kinase-independent manner has been described for several GPCRs with varied couplings: adenosine type 1 receptor and  $\mu$ -opioid receptor,<sup>7</sup> prostaglandin E2 receptor,<sup>8</sup> histamine H1 and H2 receptors (H1R and H2R),<sup>9,10</sup> lysophosphatidic acid (LPA1) receptor,<sup>11</sup> endothelin receptor type A and B,<sup>12,13</sup> follicle-stimulating hormone receptor,<sup>14</sup> and D2 dopamine receptor<sup>15</sup> among many others. In some cases, expression of the RH domain of GRK2 resulted sufficient for attenuating receptor signaling.<sup>3,16</sup>

Numerous pathologies are associated with GRK2 dysregulation, most with unsatisfied clinical demand. Increased activity of GRK2 is involved in the development and progression of cardiac hypertrophy, hypertension, heart failure, obesity, and insulin resistance in human patients or animal models.<sup>17-20</sup> Preclinical evaluations revealed a cardioprotective effect for GRK2 genetic deletion or pharmacological inhibition in cardiovascular and metabolic diseases.<sup>21</sup> Furthermore, the description of GRK2 as a therapeutic target for the treatment of Alzheimer's disease, cystic fibrosis, and rheumatoid arthritis<sup>22-24</sup> contributed to the growing interest in obtaining GRK2 inhibitors. Although the bibliography describes several molecules with inhibitory properties on GRK2 directed to its kinase domain, they did not reach advanced development stages due to their lack of specificity.<sup>25,26</sup>

In a previous publication, we showed the results of a docking-based virtual screening (DBVS) directed to the less explored RH domain of GRK2. We identified inhibitors of the desensitization of a  $G_{\alpha q}$  coupled receptor.<sup>27</sup> In this report, we identified candidates that inhibited the desensitization of a  $G_{\alpha s}$  coupled receptor, GRK2 translocation to the plasma membrane, and GRK2- $G_{\alpha s}$  coimmunoprecipitation. This will contribute to obtaining novel drug candidates with the ability to interfere with phosphorylation independent actions of GRK2 that may be useful for the treatment of pathological conditions where this protein plays a key role. Also, it brings to disposition new pharmacological tools to be applied in the research of diseases and conditions whose development or progression might be associated with GRK2.

## 2 | MATERIALS AND METHODS

### 2.1 | Cell culture

HEK293 (Human embryonic kidney, ATCC<sup>®</sup> CRL-1573), HEK293T (Human embryonic kidney, ATCC<sup>®</sup> CRL-3216), HepG2 (human hepatocellular carcinoma epithelial cells ATCC # HB-8065), and HeLa (human cervix adenocarcinoma epithelial cells, ATCC # CCL-2) cells were cultured in Dulbecco's modified Eagle's medium (DMEM) and U937 (human histiocytic lymphoma promonocytic cells ATCC # CRL-1593.2) in RPMI 1640 medium, all supplemented with 10% fetal calf serum and 50mg/ml gentamicin. HEK293 GRK2 stable clones' medium was also supplemented with 0.8 mg/ml geneticin and/or 50  $\mu$ g/ml zeocin as corresponds. HEKT Epac-SH187 medium was also supplemented with 50  $\mu$ g/ml zeocin. Cultures were maintained at 37 °C in a humidified atmosphere containing 5% CO<sub>2</sub>.

### 2.2 | Transient and stable transfections

For transient transfections, HEK293T, HeLa, and HEKT Epac-SH187 cells were grown to 80%-90% confluency. cDNA constructs were transfected into cells using K2 Transfection System (Biontex, Munich, Germany). The transfection protocol was optimized as recommended by the supplier. All assays were performed 48 h after transfection.

HEK293 clones stably expressing H2R were obtained using LipoFectamine 2000 (Invitrogen). Twenty-four hours after transfection with pcDNA3.1 Zeo (+) HA-H2R plasmid, cells were seeded in the presence of 50  $\mu$ g/ml zeocin, and clonal selection was carried out in 96-well plates for 2 weeks. Clones were tested for H2R by cAMP response assays and [<sup>3</sup>H]-tiotidine binding assays and selected to perform a second stable transfection with pcDNA3-GRK2-K220R or pcDNA3-GRK2-K220R/R106A. Cells were seeded in the presence of 1.2 mg/ml geneticin and clonal selection was carried out in 96-well plates for 2 weeks.

Stable HEK293T expressing pcDNA3.1/Zeo(1)-mTurquoise2-EPAC-cp173 Venus-Venus (Epac-SH187) (HEKT-Epac-SH187) cells

were obtained by transfection of HEK293T using K2 Transfection System (Biontix, Munich, Germany). Twenty-four hours after transfection, cells were seeded in the presence of 25 µg/ml zeocin for 2 weeks, and clonal selection was carried out in 96-well plates for 2 weeks. Clones were tested for Epac-SH187 by fluorescence spectra (450–650 nm) measurements in a FlexStation 3 Multi-Mode Microplate Reader (Molecular Devices) with excitation at 430 nm. The HEK293T Epac-SH187 clone with higher fluorescence emission was chosen for further experiments.

### 2.3 | Radioligand binding assays

$7 \times 10^4$  cells/well were seeded in 48-well plates and the day after saturation studies were performed by incubating them for 40 min at 4°C with increasing concentrations of [<sup>3</sup>H]-tiotidine (75 Ci/mmol). The incubation was stopped by rapid washing with ice-cold physiologic solution (0.9% NaCl). After three washes, the bound fraction was collected in 200 µl of ethanol, and Optiphase HiSafe3 scintillation cocktail was added to each fraction for counting in a HIDEX 300 SL counter. Two replicates per condition were performed in each independent experiment. The kinetic studies performed with 2 nM [<sup>3</sup>H]-tiotidine at 4°C showed that the equilibrium was reached at 30 min and persisted for 4 h (data not shown). Experiments on intact cells were carried out at 4°C to avoid ligand internalization.

### 2.4 | Western blot

Cells were lysed in 50 mM Tris-HCl pH 6.8, 2% SDS, 100 mM 2-mercaptoethanol, 10% glycerol, and 0.05% bromophenol blue and sonicated to shear DNA. Total cell lysates were resolved by 12% SDS-PAGE. Blots were incubated with primary anti-tubulin and anti-GRK2 antibodies (Santa Cruz Biotechnology, CA; see the “Materials and methods” section for more details), followed by horseradish peroxidase-conjugated anti-rabbit antibodies (Vector Laboratories, CA; see the “Materials and methods” section for more details) and developed by enhanced chemiluminescence (ECL) following the manufacturer's instructions (Amersham Life Science, England).

### 2.5 | cAMP response assays

For concentration curves, assays clones were seeded in 48-well plates. The day after, they were incubated for 3 min in a basal culture medium supplemented with 1mM IBMX at 37°C, and stimulated with increasing concentrations of amthamine (Amtha) for 10 min.

For response assays in the presence of candidates, clones were seeded in 48-well plates. The day after, they were pretreated for 40 min with 10 µM or 100 µM of each compound or equivalent amount of DMSO, incubated 3 min in basal culture medium supplemented with 1 mM IBMX at 37°C, and stimulated with 10 µM Amtha for 10 min.

Reactions were stopped by ethanol addition followed by centrifugation at 3000× *g* for 5 min. The ethanol phase was then dried, and the residue resuspended in 50 mM Tris-HCl pH 7.4, 0.1% BSA. cAMP content was determined by the competition of [<sup>3</sup>H]-cAMP for PKA in a cAMP radiobinding protein assay, as previously described.<sup>6</sup> Two replicates per condition were performed in each independent experiment.

FRET time-course of cAMP intracellular levels was measured as previously described.<sup>28</sup> Briefly, HEK293T Epac-SH187 transfected with pCEFL-H2R were seeded in 96-well plates at a density of  $10^5$  cells/well. To measure H2R desensitization, cells were treated with amthamine for 1 h in the presence of different concentrations of C3Z392 ranging from 30 nM to 100 µM. Before starting each experiment, cells were washed with NaCl 0.9% twice and 100 µl of FluoroBrite DMEM (Thermofisher) was added to each well before placing the plate in a FlexStation<sup>®</sup>3 (Molecular Devices) at 37°C. In order to determine cAMP response, we measured the baseline fluorescence signal detected at 475 nm (donor) and 530 nm (FRET) emission with excitation at 430 nm. Using the onboard pipettor, we added 50 µl of amthamine after 40 s and then monitored the signal every 20 s for a total of 600 s. FRET and donor intensities were measured for each time point. FRET/donor ratio was calculated and normalized to basal levels—before stimulation—(R/R<sub>0</sub>) for each time point. An AUC value of 10-minute R/R<sub>0</sub> cAMP response was calculated for each replicate. The concentration–response curve was constructed by plotting AUC values of 10-minute R/R<sub>0</sub> cAMP response versus log [C3Z392].

### 2.6 | GRK2 translocation assay

HeLa cells were seeded in 35 mm plates and transfected with pEGFP-HA-GRK2 (45-178) GFP alone or in combination with pcDNA3.1Zeo (+) HA-H2R. After 24 h, cells were seeded in polylysinated glass at 15% confluence and 24 h later cells were starved for 4 h and then treated with 10 µM Amtha for 10 min, with compounds at 100 nM for 30 min or equivalent condition of DMSO as indicated. Cells were then washed with PBS, fixed in 4% paraformaldehyde in PBS for 15 min, and washed again. Images were obtained using an Axio Observer.Z1 microscope (Carl Zeiss Microscopy GmbH, Germany; Objective LCI Plan-Neofluar 63x/1,30 Imm Korr DIC M27; Optovar 1x Tubelens; ZEISS Filter set 38 HE-eGFP, BP 470/40, FT 495, BP 525/50, and AxioCam HRm3 S/N 631 camera (adaptor 0,63x; exposure time 500–900 ms; focus 0,86 µm). Intensity profiles were performed using Image J software.

### 2.7 | GRK2-gas coimmunoprecipitation

HEK293T cells plated in 100 mm dishes were co-transfected with pCEFL-H2R, pcDNA3-GRK2-K220R, and pcDNA3-HA-G<sub>α</sub>s or not for non-specific precipitation control as indicated. Forty-eight hours after transfection, cells were starved for 1 h, washed with

PBS, and incubated at 37°C with 10  $\mu$ M amthamine for 10 min or indicated compounds at 100 nM for 30 min. Cross-linking was done in intact cells by replacement of treatment with 3 ml of PBS/2.5 mM dithiobis(succinimidyl propionate) (DSP) (Pierce) with 10  $\mu$ M amthamine, 100 nM compound and incubation for 30 min at 25°C. DSP was washed with PBS and cells were solubilized in 1 ml of radioimmunoprecipitation assay (RIPA) buffer (1% Nonidet P-40, 0.5% sodium deoxycholate, 0.1% SDS, 50 mM Tris pH 7.4, 100 mM NaCl, 2 mM EDTA, 50 mM NaF, 1 mM phenylmethylsulfonyl fluoride, 5  $\mu$ M aprotinin, 10  $\mu$ M leupeptin, 5  $\mu$ M pepstatin, 1 mM sodium vanadate). Next, the samples were homogenized, and the lysates were centrifuged for 15 min at 12 000 $\times$  g and 4°C. An aliquot was taken from the supernatant, and Laemmli buffer was added (INPUT). The remaining supernatant was added to agarose beads coupled to anti-HA antibody and incubated ON with rotation at 4°C. Next, samples were centrifuged for 2 min at 2000 $\times$  g and 4°C, washed four times with lysis buffer, and the pellet was resuspended in Laemmli buffer (IP). Separation of immune complexes and cleavage of the cross-linker was done through 5 min incubation at 100°C. Immunoprecipitated proteins were resolved by SDS-PAGE and transferred to nitrocellulose membranes. HA-G $\alpha$ s and GRK2 were detected with a rabbit anti-HA antibody, rabbit anti-G $\alpha$ s antibody, or rabbit anti-GRK2 antibody as described below.

## 2.8 | Cytotoxicity assays

HepG2 and U937 cells were treated with increasing concentrations, ranging from 333 nM to 100  $\mu$ M, of C2Z858, C3Z392, C4Z102, C5Z299, or DMSO for 48 h in 96-well plates. For HEPG2 cells supernatants were collected, cells were incubated with trypsin, and fractions were combined and centrifuged. The pellet was incubated for 5 min with a 0.4% solution of trypan blue. For the U937 line, cells were resuspended, and an aliquot was incubated for 5 min with a 0.4% solution of trypan blue. The proportion of non-viable cells (blue/blue + white) was determined by counting in a Neubauer chamber.

## 2.9 | Log Kw determination

Experimental logarithms of capacity factor ( $\log k$ ) were calculated by liquid chromatography (HPLC, Waters 590 HPLC Pump) with an ultraviolet detector (320–336 nm, Jasco-975, Software WinPcChrom XY, Jasco Inc) and a Sunfire column C18, 5.0 mm, 4.6  $\times$  150 mm (Waters Corp.). Stock solutions of each in DMSO (3.5 mg/ml) were injected (10 ml) and a mobile phase composed of acetonitrile–buffer phosphate pH 7.0 (29 mM) of different volume ratios (20:80, 25:75, 30:70, 40:60, 45:55, 50:50, and 55:45) was pumped at a flow rate of 1.0 ml/min. Logarithms of capacity factor ( $\log k$ ) were calculated as follows:

$$\text{Log}k = \log \left[ (t_r - t_o) / t_o \right]$$

where  $t_r$  and  $t_o$  are the retention time and the dead time (solvent front, DMSO), respectively. A curve of  $\log k$  versus the percentage of acetonitrile (%) in the mobile phase was built and  $\log k_{\text{water}}$  ( $\log k_w$ ) values were extrapolated at 0% acetonitrile.<sup>29</sup>

## 2.10 | Data and statistical analysis

Numbers (n) for all experiments are provided in corresponding figure legends and refer to independent measurements. Data are presented as mean  $\pm$  standard deviation (SD). Fittings of sigmoidal concentration-response and binding saturation assay were performed with GraphPad Prism 6.00 for Windows, GraphPad Software (San Diego, CA). In radioligand binding assays specific binding was calculated by subtraction of nonspecific binding from total binding. For western blot data analysis, films were scanned and quantified using ImageJ software from National Institutes of Health (NIH) for the densitometry analysis of bands. For quantification, the background value of the scanned gel was subtracted, and the relative abundance was achieved by relativizing GRK2 content to  $\beta$ -tubulin. Relative abundance was then normalized to control H2.1 clone.

Statistical analysis was carried out by one-way ANOVA followed by Bonferroni post-test or two-way ANOVA followed by Dunnett's post-test. Post hoc tests were run only if overall statistically significant difference between means were obtained. Statistical significance was accepted when  $p < .05$ . Statistics were performed using GraphPad 6.00 for Windows, GraphPad Software (San Diego, CA).

## 2.11 | Materials

Cell culture medium, antibiotics, isobutyl methylxanthine (IBMX), cAMP, bovine serum albumin (BSA), and anti-HA-agarose beads were obtained from Sigma Chemical Company (St. Louis, MO). Dithiobis(succinimidyl propionate) (DSP) was from Pierce (Rockford, USA). [<sup>3</sup>H]-cAMP, [<sup>3</sup>H]-tiotidine, and Optiphas HiSafe3 scintillation cocktail were purchased from Perkin Elmer Life Sciences (Boston, MA), and amthamine was purchased from Tocris Cookson Inc (Ballwin, MO). Fetal bovine serum was purchased from Natocor (Córdoba, Argentina). Other chemicals used were of analytical grade and obtained from standard sources.

pcDNA3 GRK2-K220R and pcDNA3 GRK2-R106A/K220R were a kind gift from Dr. J. Benovic (Thomas Jefferson University, Microbiology and Immunology Department, Kimmel Cancer Center, Philadelphia). pEGFP-HA-GRK2 (45-178) GFP was a generous gift from Dr. P. Wedegaertner, (Thomas Jefferson University, Philadelphia, USA). pCEFL-H2R and pCEFL-HA-H2R were obtained as previously reported.<sup>10</sup> Sequence coding for HA-H2R was subcloned into the *HindIII/XbaI* site of pcDNA3.1Zeo(+) (Thermo Fisher Scientific). Restriction enzymes were obtained from Takara Co. Ltd, Shiga, Japan.

Protein A/G Plus-Agarose (catalog #SC-2003/Lot #J0118/Santa Cruz Biotechnology, CA). Primary antibodies anti-HA (IgG from rabbit/catalog #SC-805/Lot #K1915/final dilution: 1/500), anti- $\beta$ tubulin antibody (IgG from rabbit/catalog #SC-9104/Lot #F1210/final dilution: 1/500), and anti-GRK2 antibody (IgG from rabbit/catalog #SC-562/Lot #F1610/final dilution: 1/1000) were purchased from Santa Cruz Biotechnology, CA. Secondary anti-rabbit antibody (IgG from goat/catalog #PI1000/Lot #X0126/final dilution: 1/4000) was purchased from Vector Laboratories (CA).

### 3 | RESULTS

#### 3.1 | Screening of compounds in cellular models

In a previous report, we described a DBVS approach based on the RH domain of GRK2 as a molecular target to search for potential inhibitors of the interaction between GRK2 and  $G\alpha$  protein. From the hit list purchased from the supplier Enamine, we found a set of molecules able to enhance calcium signaling ( $G\alpha_q$ -coupled).<sup>27</sup> In the present work, we aimed to test the hit list on their ability to inhibit GRK2 action over  $G\alpha_s$  signaling.

To carry out the *in vitro* evaluation of the compounds over cAMP response, we designed a suitable biological model consisting of stable clones of HEK293 overexpressing different GRK2 variants and the histamine H2 receptor (H2R), which is susceptible to desensitization by RH domain of GRK2.<sup>10</sup> On one hand, the "Probe system" was obtained by overexpressing the H2R and a variant of GRK2 unable to phosphorylate, but with conserved RGS activity (GRK2-K220R). On the other hand, the "Control system" was obtained by cotransfecting the cells with plasmids coding for H2R and for a variant of GRK2 that besides the kinase mutation presents its RGS activity abolished (GRK2-R106A/K220R). After cell transfection with H2R and clonal selection with 1.2 mg/ml geneticin, cAMP response assays to the specific H2 agonist Amtha were performed. From the three clones evaluated, H2.1 presented increased basal and stimulated cAMP production with respect to control (Figure 1A, left panel). Radioligand-binding experiments using [<sup>3</sup>H]-tiotidine were performed to confirm H2R overexpression (Figure 1A, right panel). An increase in binding sites was observed with a  $B_{max}$  ranging from  $290 \pm 97$  sites in control HEK293 cells to  $4684 \pm 191$  sites in the H2.1 clone. Next, H2.1 clone was transfected alternatively with GRK2-K220R to generate the probe system, or GRK2-R106A/K220R to generate the control system, and cells were grown with 50  $\mu$ g/ml zeocin for clonal selection. GRK2 variants overexpression was verified through western blot (Figure 1B, upper panel) and those clones with higher GRK2 levels were chosen to perform concentration-response curves to Amtha in order to validate systems behavior. Probe system clones presented a lower cAMP response with respect to control H2.1 cells ( $R_{max_{K3}} = 10.8 \pm 1.2$  pmol,  $R_{max_{K7}} = 7.3 \pm 0.4$  pmol,  $R_{max_{H2.1}} = 20.5 \pm 1.4$  pmol;  $p < .05$ , F test), due to exacerbated H2R desensitization caused by the overexpression of a functional

RH domain. Conversely, Control system clones presented a higher response ( $R_{max_{KR5}} = 65.2 \pm 9.1$  pmol,  $R_{max_{KR10}} = 72.3 \pm 7.7$  pmol,  $R_{max_{H2.1}} = 20.5 \pm 1.4$  pmol;  $p < .05$ , F test), consistent with the expression of a dominant negative GRK2 variant unable to desensitize the receptor (Figure 1B, lower panel).

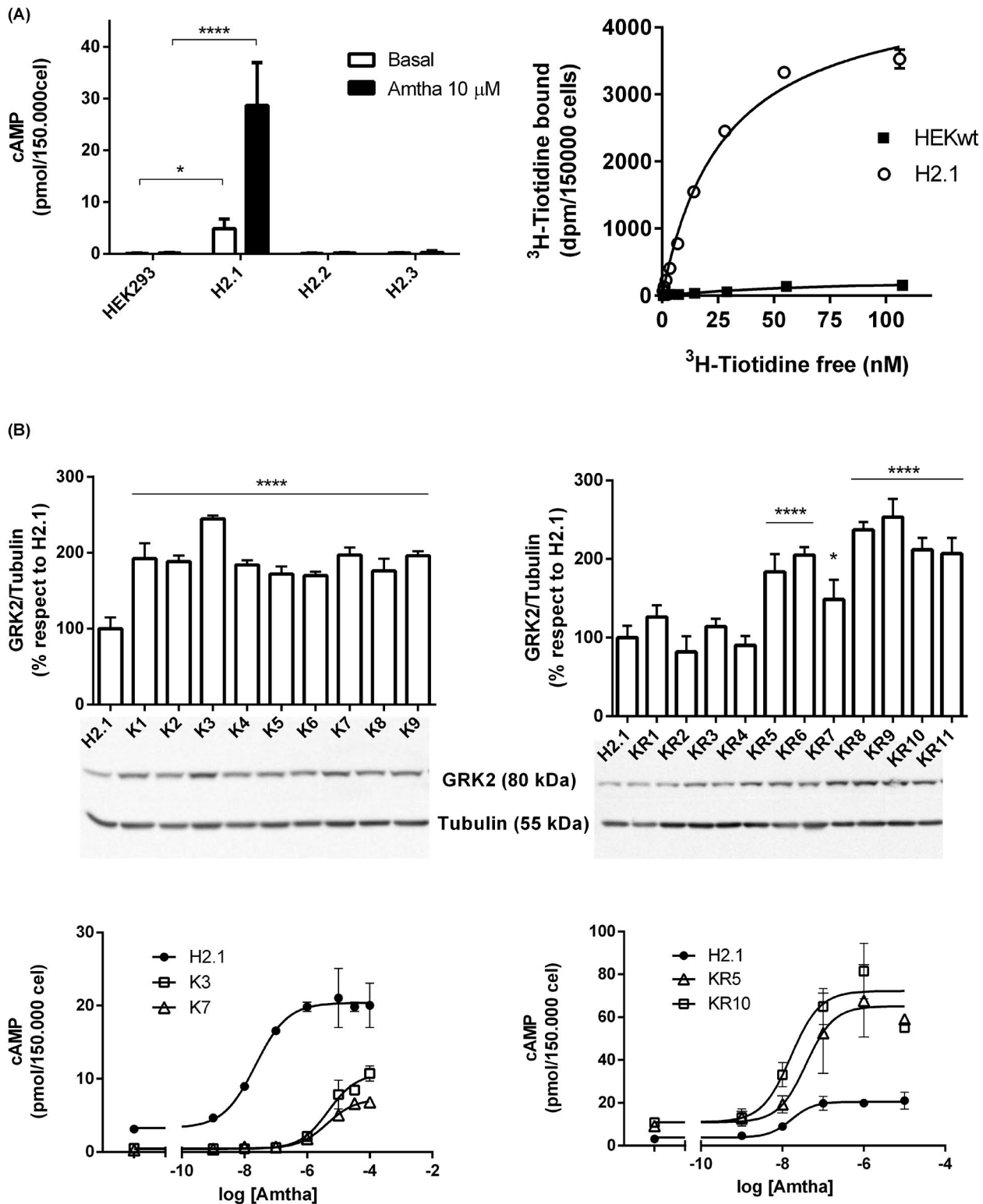
These cellular systems were used in screening format assays, in which compounds listed in Table 1 were evaluated for their ability to enhance H2R cAMP response to the agonist. To carry out the biological activity screening, both cell systems were pretreated for 40 min with 10 and 100  $\mu$ M of the selected compounds. Vehicle control was performed by pretreating the cells with an equivalent volume of DMSO. Next, cells were stimulated with 10  $\mu$ M Amtha in the presence of 1 mM IBMX and cAMP levels were determined.

Compounds C1Z392, C2Z858, C3Z392, C4Z102, and C5Z299 increased significantly H2R cAMP response in the RGS system as compared to vehicle control (Figure 2A). However, C1Z392 also increased H2R response in Control system where the RH domain is not functional, indicating a non-specific effect of this compound over another target involved in cAMP pathway different from the RH domain of GRK2 (Figure 2B). None of the compounds have a significant effect over cAMP basal levels at the tested concentrations nor showed statistically significant differences between 10  $\mu$ M and 100  $\mu$ M concentrations (Figure 2). Although the lack of effect Control system supports some selectivity of action, we cannot rule out the possibility that these compounds present off-target effects that could not be detected with our read-out assay.

#### 3.2 | Preliminary ADMET evaluation of active compounds

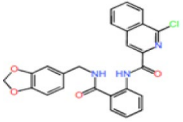
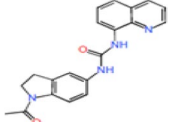
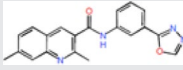
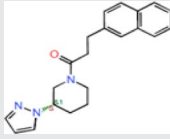
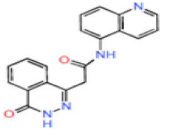
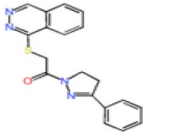
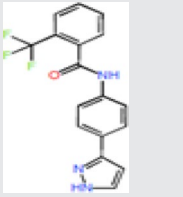
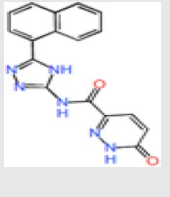
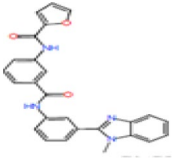
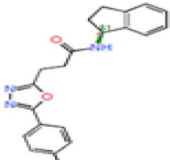
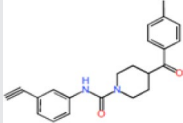
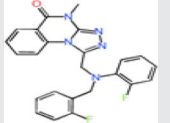
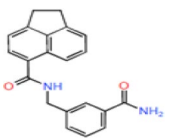
To obtain a preliminary evaluation of ADMET properties (Absorption, Distribution, Metabolism, Elimination, Toxicity) of the compounds, we evaluated their potential systemic and hepatic toxicity *in vitro* employing promonocytic U937 and hepatocyte HEPG2 human cells. To perform cytotoxicity assays, cells were incubated for 48 h with the inhibitors, in concentrations ranging from 0.33  $\mu$ M to 100  $\mu$ M. We analyzed cell viability using the trypan blue exclusion method and Neubauer chamber counting. It should be noted that it was not possible to test higher concentrations due to limited solubility of the compounds in aqueous medium. Results showed that in U937 line, only 100  $\mu$ M C4Z102 induced significant cell death with respect to control with DMSO (10% of total cells,  $*p < .05$ , Bonferroni test), with a  $pEC_{50} = 4.76 \pm 1.76$  (Figure 3A, left panel). On the other hand, in HEPG2 line only C2Z858 at all the concentrations tested showed significant toxicity with respect to control with a  $pEC_{50} = 4.98 \pm 1.1$  (100  $\mu$ M  $***p < .005$ , 50  $\mu$ M  $**p < .01$ , other  $*p < .05$ , Bonferroni test) (Figure 3A, right panel).

We also tested compounds lipophilicity, through the determination of their experimental log  $K_w$ , which reflects the logP of a molecule. Compounds were individually injected into an RP-HPLC system, and due to their differential interaction between the stationary phase and the variable ACN/buffer proportion mobile phase,



**FIGURE 1** Obtention and characterization of probe and control systems. (A) HEK293 control cells or clones transfected with pCDNA3.1 Zeo (+) H2R and resistant to zeocin (H2.1, H2.2, and H2.3) were evaluated for cAMP response after stimulation with 10  $\mu$ M amthamine (Amtha) in the presence of IBMX (left panel) and by saturation binding assay with [<sup>3</sup>H]-tiotidine (right panel) as detailed in the "Materials and methods" section. Data were analyzed by two-way ANOVA and Dunnett's post-test. \* $p < .05$ ; \*\*\*\* $p < .0001$ . (B) H2.1 clone was transfected with pcDNA3-GRK2K220R (left panel) or pcDNA3-GRK2K220R/R106A (right panel) and the clones resistant to geneticin were analyzed for GRK2 overexpression by SDS-PAGE and western blot. Data were analyzed by one-way ANOVA and Dunnett's post-test. \* $p < .05$ ; \*\*\*\* $p < .0001$ . (C) Probe system (left panel) and control system (right panel) were exposed for 10 min to increasing concentrations of Amtha at 37 °C in the presence of 1 mM IBMX. cAMP levels were determined as detailed in the "Materials and methods" section. Data represent the mean  $\pm$  SD of assay duplicates. Similar results were obtained in three independent experiments

TABLE 1 Compounds were evaluated for their ability to enhance H2R cAMP response to the agonist

Compound	Identifier code	Chemical structure	Compound	Identifier code	Chemical structure
C1Z392	Z392135950		C2Z858	Z858318340	
C3Z392	Z392685436		C4Z102	Z1023979890	
C5Z299	Z29903317		C6Z298	Z298486826	
C7Z646	Z646217568		C8Z822	Z822250674	
C9Z817	Z817596858		C10Z169	Z169793274	
C11Z745	Z745925938		C12Z114	Z1143364625	
C13Z343	Z343504030				

Note: Chemical structures and identifier code (Z) of compounds are shown.

a retention time (RT) for each of the mixtures of increasing polarity was obtained. RTs were processed as described in the "Materials and methods" section to obtain log Kw values for C2Z858:  $1.87 \pm 0.29$ , C3Z392:  $1.58 \pm 0.26$ , C4Z102:  $2.49 \pm 0.42$ , and C5Z299:  $1.63 \pm 0.57$  (Figure 3B).

### 3.3 | Confirmation of the mechanism of action of active compounds

In basal conditions, GRK2 is located uniformly in the cytosol of the cell. However, when receptors are activated, GRK2 is translocated to plasma membrane.<sup>5,30</sup> This behavior was also observed for the RH domain of GRK2 fused to GFP (GRK2 (45-178) GFP) in

colocalization experiments with a constitutively active Gαq protein.<sup>27</sup> Therefore, to delve into the inhibitors' mechanism of action, we evaluated their effect on the translocation of GRK2 RH domain. For this evaluation, we employed HeLa cells transiently transfected with a plasmid coding for GRK2 (45-178) GFP, or co-transfected with plasmids coding for GRK2 (45-178) GFP and H2R. Then, cells were treated, or not, with 10 μM Amtha for 3 min, fixed, and analyzed by confocal microscopy. We observed that GRK2 (45-178) GFP is located in the cytoplasm but, when H2R is overexpressed, the fluorescence signal becomes intensified in the plasma membrane. Presumably, given the high constitutive activity of the receptor<sup>31</sup> GRK2 redistribution occurs even in the absence of the agonist (Figure 4A). For compound evaluation, transfected cells were incubated for 30 min with 100 nM of the active compounds

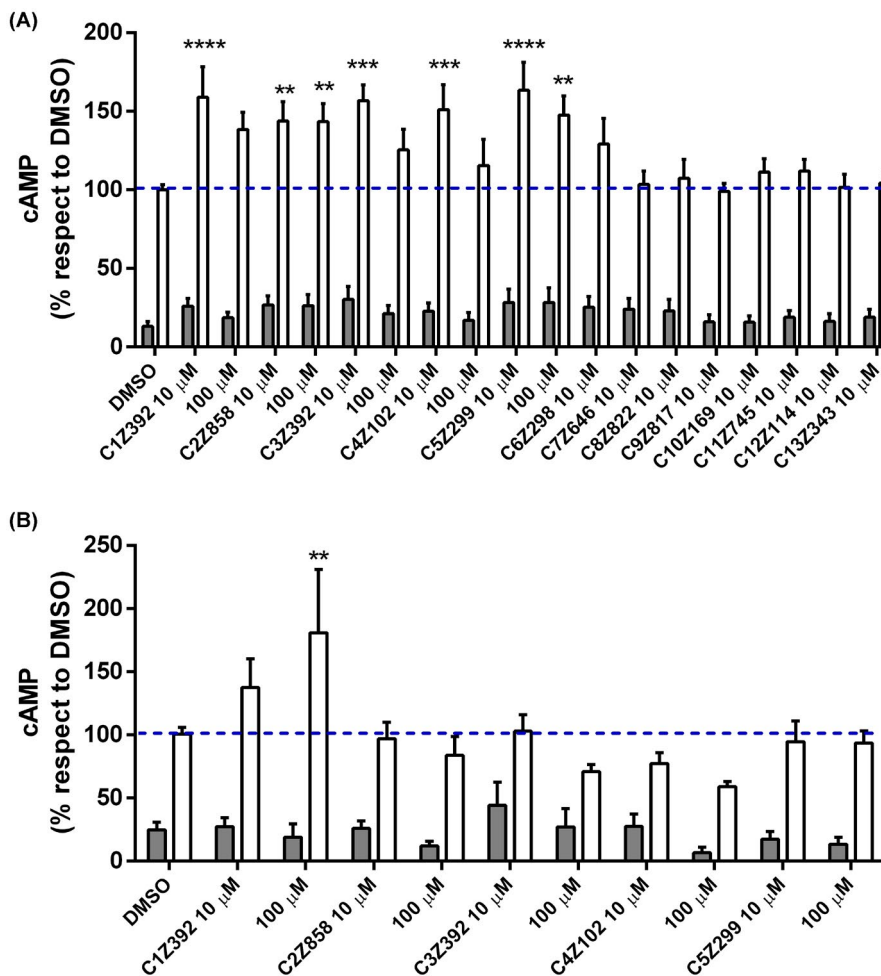


**FIGURE 2** Biological activity of hit compounds: positive modulation of cAMP response of H2R. (A) Probe system or (B) Control system cells were pre-treated with 10  $\mu$ M or 100  $\mu$ M of indicated compounds for 40 min, and basal cAMP response or stimulated with 10  $\mu$ M amthamine (Amtha) in the presence of IBMX was determined as detailed in the “Materials and methods” section. Grey bars correspond to basal and white to the stimulated response. Data were analyzed by two-way ANOVA and Dunnett's post-test. \*\* $p < .01$ , \*\*\* $p < .001$ ; \*\*\*\* $p < .0001$  with respect to control (DMSO)-stimulated response. Data represent the mean  $\pm$  SD of assay duplicates. Similar results were obtained in three independent experiments

C2Z858; C3Z392; C5Z299, using C9Z817 as negative control, or with an equivalent amount of DMSO as vehicle control. The fluorescence intensity was quantified in each image using line intensity profiles across each one of the cells. The presence of peaks at the beginning and the end of the profile indicates the increased concentration of GRK2 (45-178) GFP at the cell margins. The relocation of RH-GRK2 to the plasma membrane due to H2R overexpression observed in the control with DMSO and in the control with the inactive compound C9Z817 was drastically dampened when cells were treated with compounds C2Z858, C3Z392, and C5Z299 (Figure 4B).

It has been described that the RH domain of GRK2 is able to interact with G proteins to avoid downstream signaling in a mechanism independent of receptor phosphorylation.<sup>5,6,30</sup> In this context, we evaluated the effect of the inhibitors on the direct interaction between GRK2 and the G $\alpha$ s protein, performing co-immunoprecipitation of both proteins in whole-cell assays. HEK293T cells were cotransfected with plasmids coding for G $\alpha$ s

protein fused to the HA epitope (HA-G $\alpha$ s), GRK2-K220R, and H2R, and protein extracts were prepared after a stimulus with 10  $\mu$ M Amtha. Subsequently, we immunoprecipitated the HA-G $\alpha$ s protein using anti-HA coupled agarose beads. Co-precipitated GRK2 was detected by Western blot in both basal and Amtha-treated cells (Figure 5A). For compound evaluation, cotransfected cells were treated with 100 nM C3Z392, C5Z299, or DMSO for 30 min and protein extracts were prepared. C3Z392 diminished the proportion of GRK2 that co-immunoprecipitated with HA-G $\alpha$ s in 36.4  $\pm$  3.3% of vehicle control and C5Z299 in 25.5  $\pm$  3.3% (Figure 5B).

### 3.4 | In vitro efficacy of active compounds

Although active and selective compounds increase receptor response, GRK membrane translocation, and impede RH G $\alpha$ s interaction, we wanted to confirm if they were able to inhibit receptor



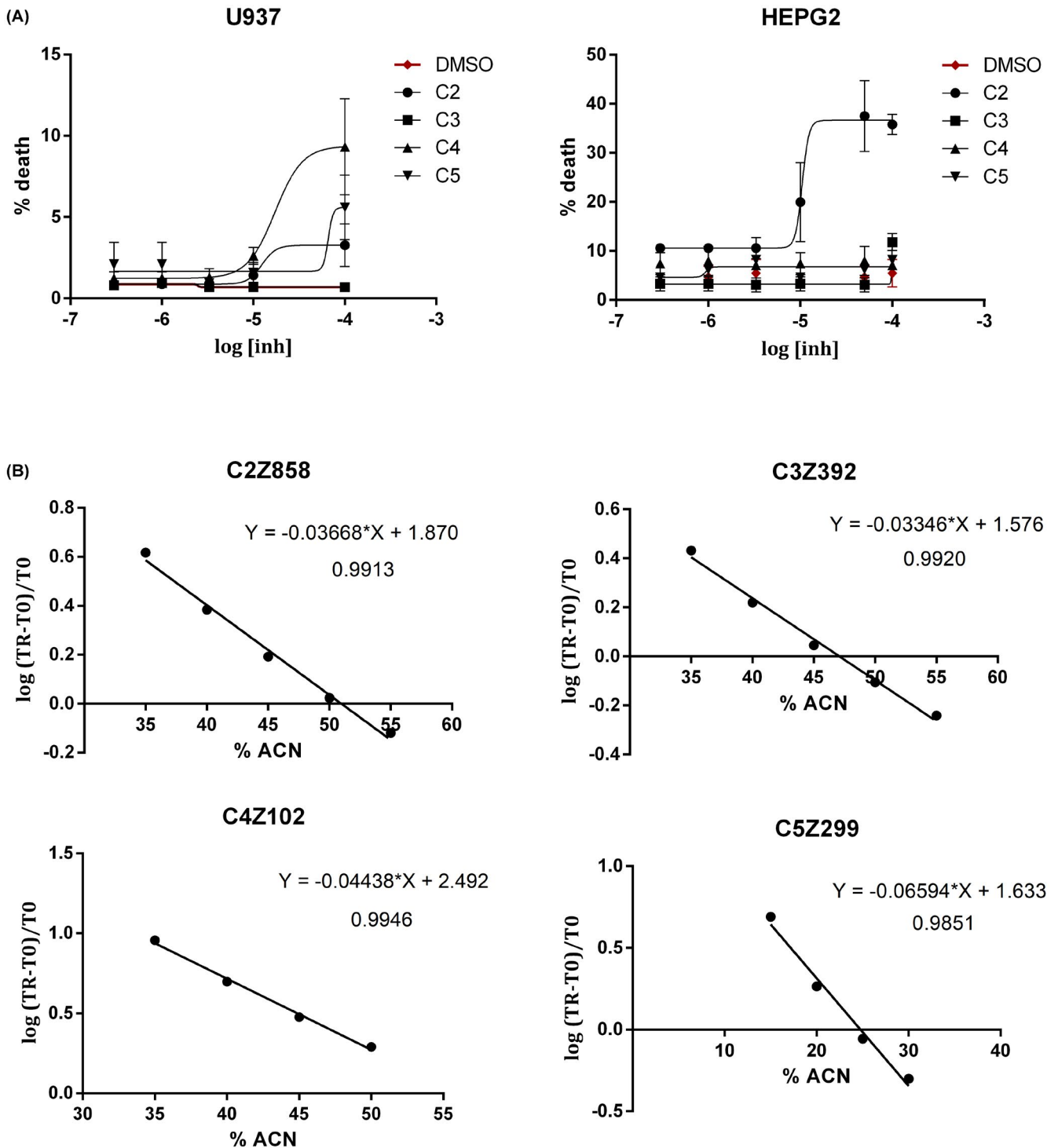


**FIGURE 3** Preliminary profiling of physicochemical and *in vitro* ADMET properties of hit compounds. (A) U937 (left panel) and HEPG2 (right panel) cells were treated with increasing concentrations of C2Z858, C3Z392, C4Z102, and C5Z299 or DMSO for 48 h, and cell viability was determined by Trypan Blue exclusion test. Data represent media  $\pm$  SD of three independent experiments. (B) Lipophilicity of hit compounds was determined by RP-HPLC as detailed in the “Materials and methods” section. Processing of retention time “RT” and dead time “T0” (solvent front, DMSO) for each compound is shown. Experimental log Kw values correspond to extrapolations at 0% acetonitrile (ACN)

desensitization in a cellular context where GRK2 and H2R were natively expressed. We pretreated U937 cells for 1 h with 10  $\mu$ M amthamine, in the presence of the active compounds C3 and C5, and

measured the capability of the system to respond to a new stimulus. In these conditions, cAMP response was diminished by about 85%. While C5Z299 was unable to modify response desensitization,

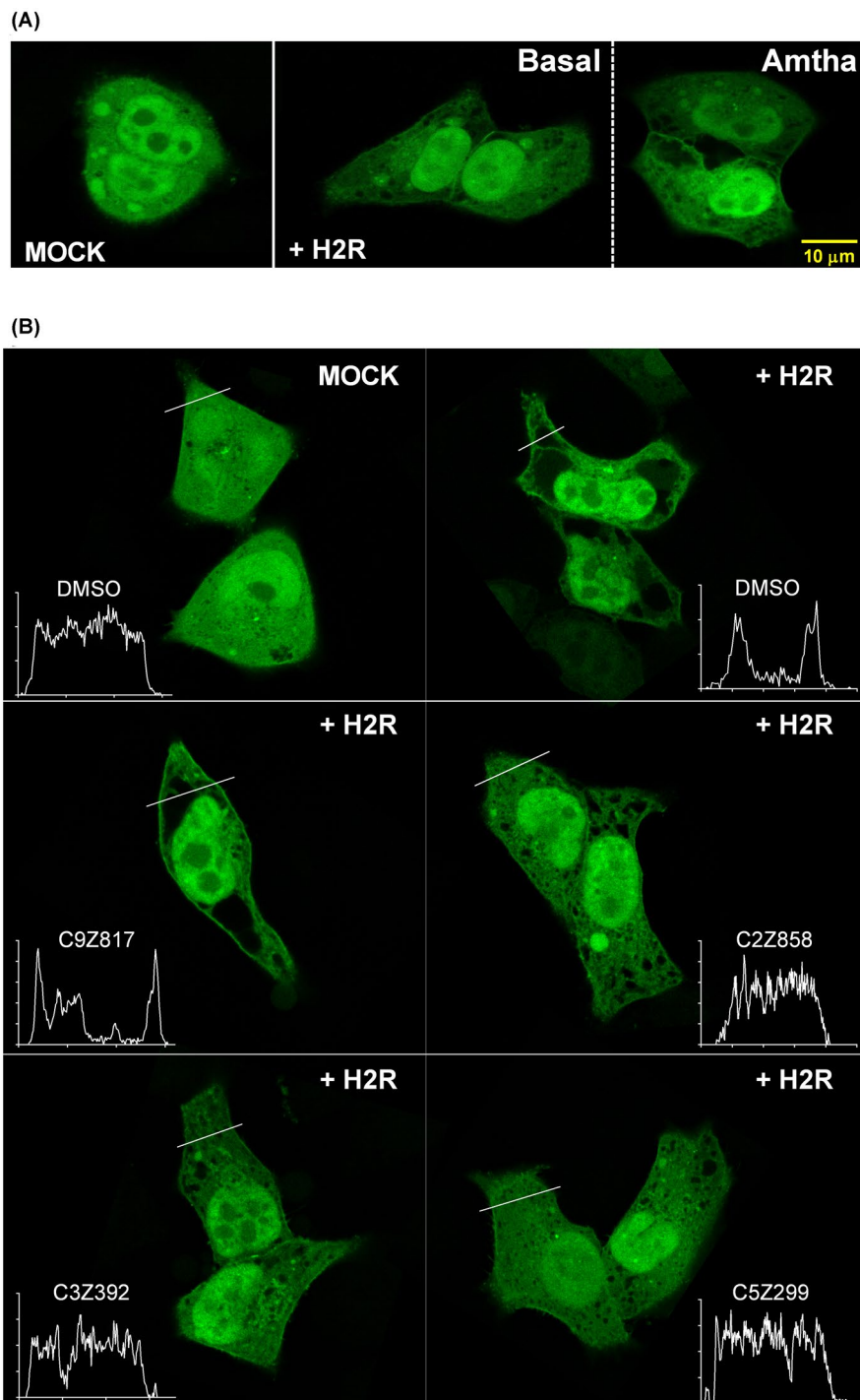


**FIGURE 4** Mechanism of action of candidates: inhibition of GRK2 (45-178) GFP translocation. (A) HELA cells were transiently cotransfected with GRK2 (45-178) GFP and H2R plasmids or empty vector (MOCK) and fixed after 48 h. Subcellular localization was assessed by confocal microscopy in basal or in 10  $\mu$ M amthamine (Amtha)-stimulated condition. (B) HELA cells were transiently cotransfected with GRK2 (45-178) GFP and H2R plasmids. Forty-eight hours after transfection cells were treated with 100 nM of C2Z858, C3Z392, C5Z299, or C9Z817 (negative control) or DMSO (vehicle control) for 40 min and fixed. At least 100 cells were examined in three independent experiments. For each cell in a given image, a line intensity profile across the cell was obtained. Representative intensity profiles are shown for each condition

C3Z392 pretreatment reduced the desensitization to 75% ( $p < .05$ ,  $t$  test) (Figure 6A). To better study the effect of C3Z392 on receptor desensitization, we developed a cell system with greater sensitivity that allows us to monitor real-time temporal progression of cAMP levels in different conditions. HEK293T cells stably transfected with the Epac-SH187 cAMP biosensor, and transiently with pCEFL-H2R, were pretreated with C3Z392 for 10 m, then treated or not with 10  $\mu$ M Amtha for 1 h, and after that restimulated. C3Z392 showed the ability to increase the residual response after receptor desensitization from  $46 \pm 6\%$  to  $73 \pm 4\%$  with a  $pEC_{50} = 7.3 \pm 0.5$

(Figure 6B,C). These results demonstrate that C3Z392 is effective in inhibiting H2 receptor desensitization in a whole-cell assay.

#### 4 | DISCUSSION

GRK2 is a protein with a confirmed therapeutic potential for several pathologies such as hypertension, heart failure, Alzheimer's, multiple sclerosis, and rheumatoid arthritis. Although its kinase domain has been extensively studied in the search for inhibitors, during the

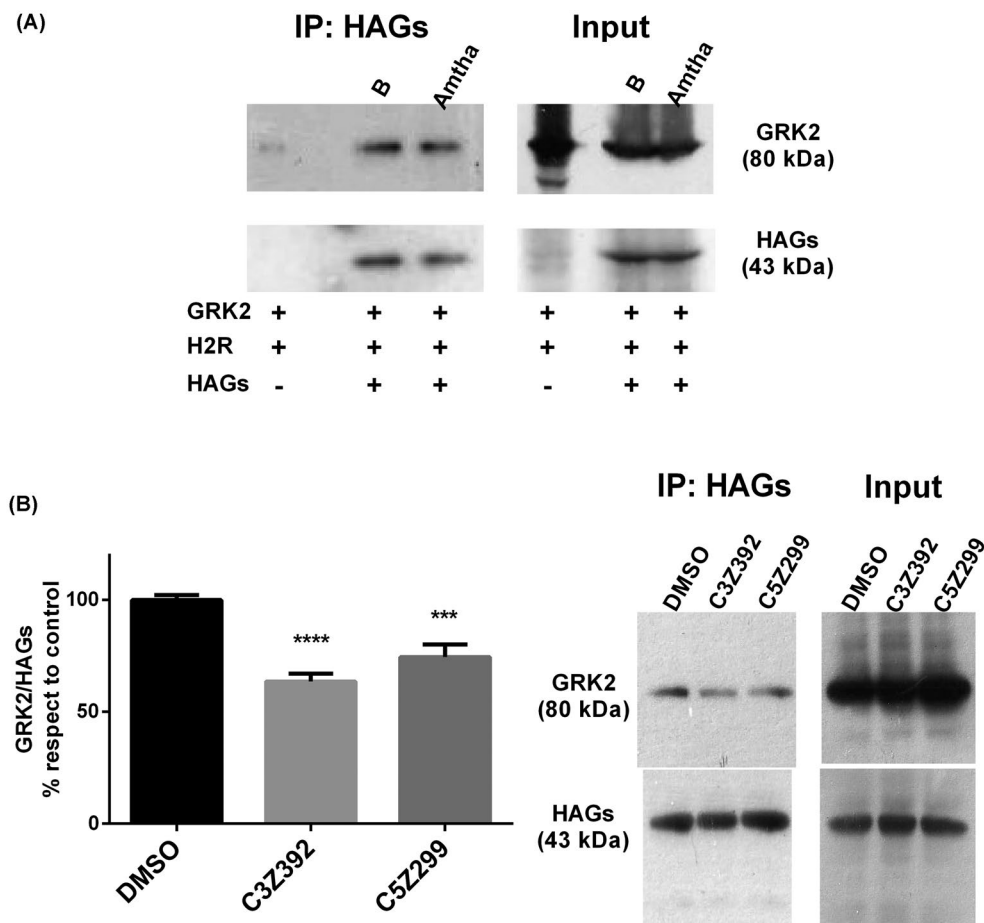


**FIGURE 5** Mechanism of action of candidates: inhibition of interaction between GRK2 and  $G\alpha_s$  subunit. Co-immunoprecipitation of  $G\alpha_s$  and GRK2 is shown. HEK293 cells co-transfected with GRK2, H2R, and HA-tagged  $G\alpha_s$ , or Mock were incubated for 10 min with 10  $\mu$ M amthamine (Amtha) (A) or treated with 10  $\mu$ M C3Z392 and C5Z299 for 30 min (B), and cross-linking with 2.5 mM dithiobis(succinimidyl propionate) was done. Cells were lysed, and HA- $G\alpha_s$  was immunoprecipitated (IP) using agarose beads coupled to anti-HA antibody. Co-precipitated GRK2 was detected by western blot using specific antibodies. Total  $G\alpha_s$  was detected by western blot using anti-HA antibodies. A representative image is shown. Densitometry analysis was performed with ImageJ as indicated in the "Materials and methods" section and analyzed by Student's *t*-test comparing GRK2 levels in candidate pre-treated versus control cells ( $n = 3$ )

past years its RGS homology domain has also been postulated as an interesting target to be modulated.<sup>6,27,32,33,34</sup> RGS family members have been under study, and several protein inhibitors have been found. For example, specific and potent (nM order) small molecule inhibitors have been described for RGS4 protein, postulated as a therapeutic target for disorders of the neurological system.<sup>35,36</sup> However, most RGS inhibitors have been identified through biochemical screening assays and have shown limited or no activity in whole-cell assays.<sup>37,38</sup> Herein, we show the novel identification of cell-active inhibitors of GRK2 RGS homology domain able to modulate  $G\alpha_s$  signaling. We developed an *in vitro* cellular screening model (Figure 1) to identify compounds that selectively modulate RH activity using dominant-negative mutants of GRK2 at its kinase or both kinase and RH domains (GRK2-R106A/K220R) that allow us to evaluate efficacy and specificity of action. Our results show that while compounds C2Z858, C3Z392, C4Z102, and C5Z299 are active and specific, C1Z392 lacks selectivity (Figure 2). However, while our experimental design allowed us to detect the undesired action of the

compounds on an element involved in the cAMP pathway other than the GRK2 RH domain, we cannot rule out the possible interaction of the compounds with targets involved in other pathways not evaluated in the present work. Nevertheless, based on our cytotoxicity studies we can assume that if occurring, those interactions do not cause cell death.

Besides efficacy, the success of a compound development is determined by its pharmacokinetic ADMET properties (Absorption, Distribution, Metabolism, Elimination, Toxicity). The unexpected toxicity of a compound is the reason why 30% of the drugs that enter drug-development pipeline development processes are unsuccessful, with hepatotoxicity being the most prominent.<sup>39</sup> Thus, we tested the cytotoxicity of the active compounds in U937 cells, to evaluate the probability that they show systemic toxicity, and in HEPG2 cells, to predict potential toxic effects in the human liver. Although all active compounds, except C2Z858, can be safely used on these systems at a concentration less than or equal to 10  $\mu$ M, C3Z392 and C5Z299 were the more innocuous

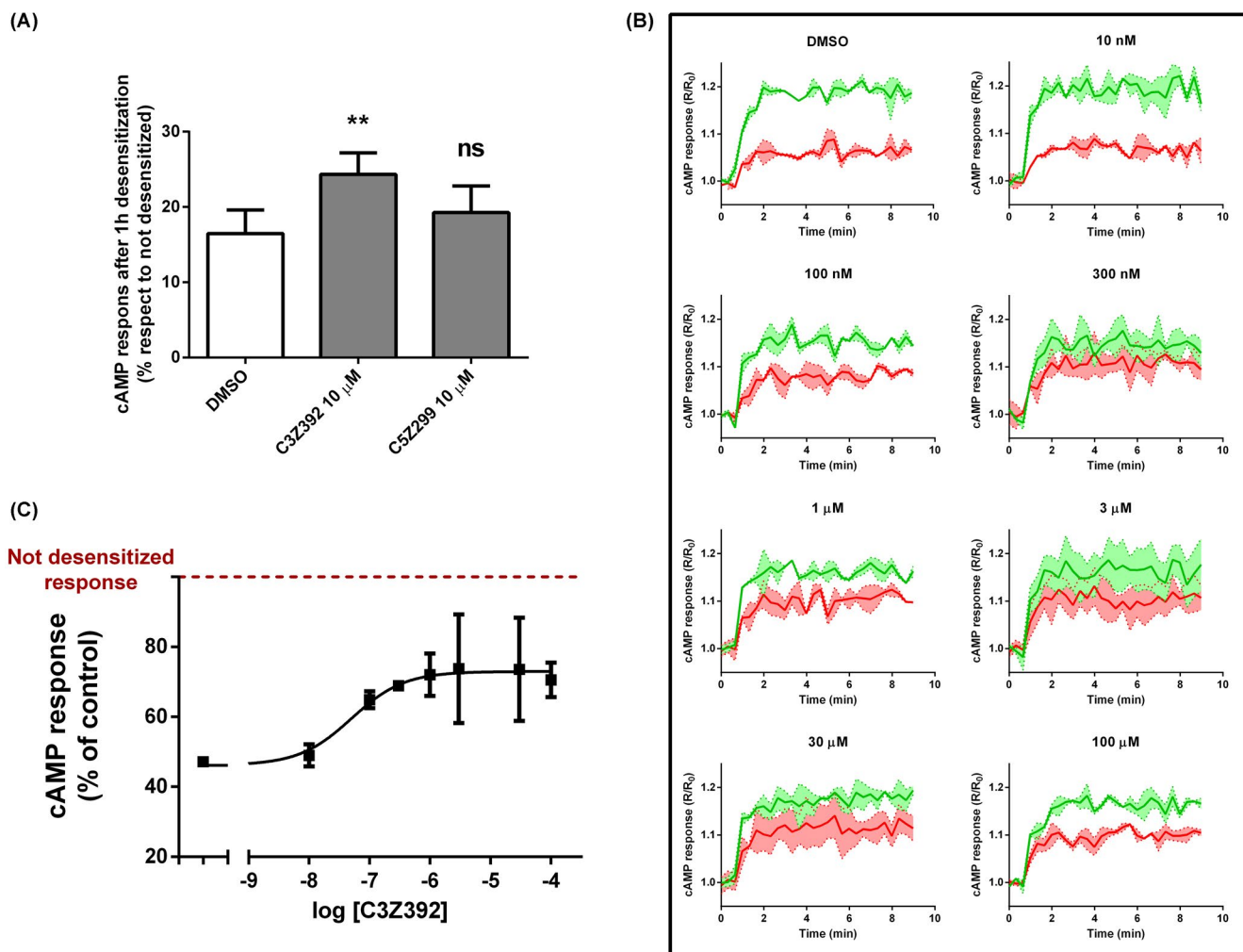


**FIGURE 6** In vitro efficacy of active compounds: inhibition of desensitization. (A) U937 cells endogenously expressing H2R and GRK2 were exposed to 10  $\mu\text{M}$  amthamine (Amtha) for 1 h and after washing, rechallenge with 10  $\mu\text{M}$  Amtha for 10 min in the presence of IBMX. cAMP response was determined as detailed in the “Materials and methods” section. Data were calculated as the means  $\pm$  SD of assay duplicates and are expressed as the ratio of stimulated over basal cAMP with respect to control (without pre-treatment) which is considered as 100%. (B) HEK293 cells transiently co-transfected with H2R and GRK2 were pre-treated during 1 h with either 10  $\mu\text{M}$  Amtha (red) or vehicle (green) in the presence of different concentrations of C3Z392 as indicated. After that, cells were washed and challenged with 10  $\mu\text{M}$  Amtha. (C) Concentration–response curves were constructed with the AUC values of 10-min R/R<sub>0</sub> cAMP response of time course of FRET changes with respect to control (without pre-treatment) determined in FlexStation<sup>®</sup>3 at 37°C as described in the “Materials and methods” section

for both the cell lines (Figure 3A). For its part, the lipophilicity of a compound refers to its ability to dissolve in fats, oils, lipids, and non-polar solvents. In vivo, it reflects its ability to be transferred from an aqueous solution to a cell membrane, and from there again to the aqueous phase of the cytosol, and to a binding site on a biological target. Therefore, lipophilicity becomes a key property that contributes to all aspects of the pharmacokinetics of a compound, and as result on its ADME properties (Absorption, Distribution, Metabolism, Elimination).<sup>40</sup> Log Kw values obtained for our compounds as lipophilicity indicators are within the optimum region that comprises values from 1 to 3<sup>40</sup> predicting adequate pharmacokinetic properties (Figure 3B).

Canonically, the GRK2 kinase domain is responsible for GPCRs desensitization. However, it was described the RH domain

involvement in receptor desensitization through a phosphorylation-independent mechanism related to its RGS function. Since RH has been shown to lack significant GTPase activating protein (GAP) activity, acceleration of G-protein GTP hydrolysis may not be its mechanism of action.<sup>4,41</sup> It has been described that the RGS family of proteins may also bind to active G $\alpha$  protein blocking downstream effector activation.<sup>42</sup> In this sense, GRK2 interaction with G $\alpha$  has been demonstrated by other groups<sup>5,30</sup> and by us (Ref. [6] and Figure 5A).

In this work, we tested a series of compounds obtained by a docking-based virtual screening employing the crystal structure of GRK2 to search for inhibitors of the protein-protein interaction (PPI) between GRK2 and G $\alpha$ .<sup>27</sup> Results from co-immunoprecipitation experiments showed that C3Z392 and C5Z299 significantly diminished the proportion of GRK2 that

co-immunoprecipitated with G $\alpha$ s, suggesting that, as expected, inhibitors' mechanism of action consists of avoiding PPI between GRK2 and G $\alpha$ s (Figure 4B). Also, the involvement of the G $\alpha$  subunit in the translocation of GRK2 to the plasma membrane in an active signaling environment has been previously demonstrated.<sup>27</sup> Herein, the co-expression of RH-GRK2 with a receptor coupled to G $\alpha$ s, such as H2R, led to a redistribution of RH-GRK2 from the cytosol to the plasma membrane (Figure 3A) that was hampered by inhibitors C2Z858, C3Z392, and C5Z299 (Figure 3B). Although the translocation inhibition by C3Z392 and C5Z299 might be due to GRK2-G $\alpha$ S PPI avoidance they have shown, RH-GRK2 binding to the receptor cannot be ruled out, and inhibitors' possible effect over this phenomenon might need further investigation. Together, these results, in addition to delving into the mechanism of action of the inhibitors, allowed us to advance in the understanding of the GRK2-mediated GPCR desensitization mechanism, in terms of less explored aspects of Gs signaling and RH modulation. This preliminary study of preclinical pharmacology of candidates allowed us to obtain useful information for their future use and optimization. In this sense, C3Z392 has been demonstrated to inhibit desensitization not only in an overexpression system but also when GRK2 and H2R were natively expressed (Figure 6), becoming the most promissory candidate.

Orthogonal assays by definition are those corresponding assays used following, or in parallel to, the primary high-throughput screening assay to confirm compound activity that is independent of the primary assay technique.<sup>43</sup> It is interesting to note that even though, just like C3Z392, C5Z299 was able to increase cAMP response and to impede RH-GRK2 translocation and GRK2 interaction with Gs, its effect on desensitization was not significant, highlighting the importance of performing orthogonal assays that converge in the candidate selection to proceed to optimization. Our results enable us to identify C3Z392 as a specific and potent GRK2 inhibitor able to impede G $\alpha$ s-coupled receptor desensitization with potency in the nM order. They also demonstrate that, beyond RH domain lack of GAP activity, this domain is a promissory target for drug development that could be used for the treatment of conditions in which exacerbated activity of GRK2 becomes pathological.

## ETHICS STATEMENT

This study was carried out using commercial cell lines, did not utilize animals nor patient identifiable data; thus, neither approval from the ethics committee nor informed consent was required.

## ACKNOWLEDGEMENTS

This study was funded by Agencia Nacional de Promoción Científica y Tecnológica (ANPCyT), PICT-2015-2443 and PICT-2019-2586; and University of Buenos Aires, UBACyT 2018 20020170200166BA01. The funding agencies have not had any involvement in the writing of the report and in the decision to submit the article for publication.

## CONFLICT OF INTEREST

The authors declare no conflict of interest.

## AUTHOR CONTRIBUTIONS

Emiliana Echeverría: Conceptualization, Validation, Formal analysis, Investigation, Writing—Original Draft, Writing—Review & Editing. Sonia Ripoll: Investigation, Writing—Review & Editing. Lucas Fabián: Investigation, Writing—Review & Editing. Carina Shayo: Conceptualization, Writing—Review & Editing, Supervision. Monczor Federico: Conceptualization, Validation, Writing—Original Draft, Writing—Review & Editing, Supervision, Funding acquisition. Fernández Natalia: Investigation, Conceptualization, Validation, Writing—Original Draft, Writing—Review & Editing, Supervision, Project administration, Funding acquisition.

## DATA AVAILABILITY STATEMENT

Data available on request from the authors.

## ORCID

Federico Monczor  <https://orcid.org/0000-0002-1113-4608>

Natalia C. Fernández  <https://orcid.org/0000-0002-8099-6471>

## REFERENCES

- Rosenbaum DM, Rasmussen SGF, Kobilka BK. The structure and function of G-protein-coupled receptors. *Nature*. 2009;459:356-363. doi:10.1038/nature08144
- Sriram K, Insel PA. G protein-coupled receptors as targets for approved drugs: how many targets and how many drugs? *Mol Pharmacol*. 2018;93:251-258. doi:10.1124/mol.117.111062
- Sallese M, Mariggio S, D'Urbano E, Iacovelli L, De Blasi A. Selective regulation of Gq signaling by G protein-coupled receptor kinase 2: direct interaction of kinase N terminus with activated galphaq. *Mol Pharmacol*. 2000;57:826-831. doi:10.1124/mol.57.4.826
- Carman CV, Parent JL, Day PW, et al. Selective regulation of Galpha(q/11) by an RGS domain in the G protein-coupled receptor kinase, GRK2. *J Biol Chem*. 1999;274:34483-34492. doi:10.1074/jbc.274.48.34483
- Day PW, Wedegaertner PB, Benovic JL. Analysis of G-protein-coupled receptor kinase RGS homology domains. In: *Methods Enzymol*. Elsevier; 2004;295-310. doi:10.1016/S0076-6879(04)90019-5
- Echeverría E, Cabrera M, Burghi V, et al. The regulator of G protein signaling homologous domain of G protein-coupled receptor kinase 2 mediates short-term desensitization of  $\beta$ 3-adrenergic receptor. *Front Pharmacol*. 2020;11:113. doi:10.3389/fphar.2020.00113
- Raveh A, Cooper A, Guy-David L, Reuveny E. Nonenzymatic rapid control of GIRK channel function by a G protein-coupled receptor kinase. *Cell*. 2010;143:750-760. doi:10.1016/j.cell.2010.10.018
- Kong G, Penn R, Benovic JL. A beta-adrenergic receptor kinase dominant negative mutant attenuates desensitization of the beta 2-adrenergic receptor. *J Biol Chem*. 1994;269:13084-13087. doi:10.1016/S0021-9258(17)36801-1
- Iwata K, Luo J, Penn RB, Benovic JL. Bimodal regulation of the human H1 histamine receptor by G protein-coupled receptor kinase 2. *J Biol Chem*. 2005;280:2197-2204. doi:10.1074/jbc.M408834200
- Fernandez N, Gottardo FL, Alonso MN, Monczor F, Shayo C, Davio C. Roles of phosphorylation-dependent and -independent mechanisms in the regulation of histamine H2 receptor by G protein-coupled receptor kinase 2. *J Biol Chem*. 2011;286:28697-28706. doi:10.1074/jbc.M111.269613
- Aziziyeh AI, Li TT, Pape C, et al. Dual regulation of lysophosphatidic acid (LPA1) receptor signalling by Ral and GRK. *Cell Signal*. 2009;21:1207-1217. doi:10.1016/j.cellsig.2009.03.011

12. Gärtner F, Seidel T, Schulz U, Gummert J, Milting H. Desensitization and internalization of endothelin receptor A. *J Biol Chem.* 2013;288:32138-32148. doi:10.1074/jbc.M113.461566
13. Steury MD, McCabe LR, Parameswaran N. G Protein-coupled receptor kinases in the inflammatory response and signaling. In *Adv. Immunol.* Elsevier; 2017;227-277. doi:10.1016/bs.ai.2017.05.003
14. Reiter E, Marion S, Robert F, et al. Kinase-inactive G-protein-coupled receptor kinases are able to attenuate follicle-stimulating hormone-induced signaling. *Biochem Biophys Res Commun.* 2001;282:71-78. doi:10.1006/bbrc.2001.4534
15. Namkung Y, Dipace C, Urizar E, Javitch JA, Sibley DR. G protein-coupled receptor kinase-2 constitutively regulates D2 dopamine receptor expression and signaling independently of receptor phosphorylation. *J Biol Chem.* 2009;284:34103-34115. doi:10.1074/jbc.M109.055707
16. Usui H, Nishiyama M, Moroi K, et al. RGS domain in the amino-terminus of G protein-coupled receptor kinase 2 inhibits Gq-mediated signaling. *Int J Mol Med.* 2000;5:335-340. doi:10.3892/ijmm.5.4.335
17. Campanile A, Iaccarino G. G-protein-coupled receptor kinases in cardiovascular conditions: focus on G-protein-coupled receptor kinase 2, a gain in translational medicine. *Biomark Med.* 2009;3:525-540. doi:10.2217/bmm.09.50
18. Lucas E, Cruces-Sande M, Briones AM, et al. Molecular pathophysiology of obesity-related diseases: multi-organ integration by GRK2. *Arch Physiol Biochem.* 2015;121:163-177. doi:10.3109/13813455.2015.1107589
19. Taguchi K, Bessho N, Hasegawa M, Narimatsu H, Matsumoto T, Kobayashi T. Co-treatment with clonidine and a GRK2 inhibitor prevented rebound hypertension and endothelial dysfunction after withdrawal in diabetes. *Hypertens Res.* 2018;41:263-274. doi:10.1038/s41440-018-0016-6
20. Ciccarelli M, Sorriento D, Fiordelisi A, et al. Pharmacological inhibition of GRK2 improves cardiac metabolism and function in experimental heart failure. *ESC Heart Fail.* 2020;7:1571-1584. doi:10.1002/ehf2.12706
21. Murga C, Arcones AC, Cruces-Sande M, Briones AM, Salas M, Mayor F Jr. G protein-coupled receptor kinase 2 (GRK2) as a potential therapeutic target in cardiovascular and metabolic diseases. *Front Pharmacol.* 2019;10:112. doi:10.3389/fphar.2019.00112
22. Obrenovich ME, Morales LA, Cobb CJ, et al. Insights into cerebrovascular complications and Alzheimer disease through the selective loss of GRK2 regulation. *J Cell Mol Med.* 2009;13:853-865. doi:10.1111/j.1582-4934.2008.00512.x
23. Mak JCW, Chuang T-T, Harris CA, Barnes PJ. Increased expression of G protein-coupled receptor kinases in cystic fibrosis lung. *Eur J Pharmacol.* 2002;436:165-172. doi:10.1016/S0014-2999(01)01625-9
24. Wang WCH, Muhlbachler KA, Bleecker ER, Weiss ST, Liggett SB. A polymorphism of G-protein coupled receptor kinase5 alters agonist-promoted desensitization of  $\beta$ 2-adrenergic receptors. *Pharmacogenet Genomics.* 2008;18:729-732. doi:10.1097/FPC.0b013e32830967e9
25. Thal DM, Homan KT, Chen J, et al. Paroxetine is a direct inhibitor of G protein-coupled receptor kinase 2 and increases myocardial contractility. *ACS Chem Biol.* 2012;7:1830-1839. doi:10.1021/cb3003013
26. Homan KT, Tesmer JGG. Molecular basis for small molecule inhibition of G protein-coupled receptor kinases. *ACS Chem Biol.* 2015;10:246-256. doi:10.1021/cb5003976
27. Echeverría E, Velez Rueda AJ, Cabrera M, et al. Identification of inhibitors of the RGS homology domain of GRK2 by docking-based virtual screening. *Life Sci.* 2019;239:116872. doi:10.1016/j.lfs.2019.116872
28. Carozzo A, Yaneff A, Gómez N, et al. Identification of MRP4/ABCC4 as a target for reducing the proliferation of pancreatic ductal adenocarcinoma cells by modulating the cAMP efflux. *Mol Pharmacol.* 2019;96:13-25. doi:10.1124/mol.118.115444
29. Glisoni RJ, Chiappetta DA, Finkielstein LM, Moglioni AG, Sosnik A. Self-aggregation behaviour of novel thiosemicarbazone drug candidates with potential antiviral activity. *New J Chem.* 2010;34:2047. doi:10.1039/c0nj00061b
30. Sterne-Marr R, Tesmer JGG, Day PW, et al. G protein-coupled receptor kinase 2/G $\alpha$ q/11 interaction. *J Biol Chem.* 2003;278:6050-6058. doi:10.1074/jbc.M208787200
31. Tubio MR, Fernandez N, Fitzsimons CP, et al. Expression of a G protein-coupled receptor (GPCR) leads to attenuation of signaling by other GPCRs. *J Biol Chem.* 2010;285:14990-14998. doi:10.1074/jbc.M109.099689
32. Usui I, Imamura T, Satoh H, et al. GRK2 is an endogenous protein inhibitor of the insulin signaling pathway for glucose transport stimulation. *EMBO J.* 2004;23:2821-2829. doi:10.1038/sj.emboj.7600297
33. Lee I-H, Song S-H, Campbell CR, Kumar S, Cook DI, Dinudom A. Regulation of the epithelial Na<sup>+</sup> channel by the RH domain of G protein-coupled receptor kinase, GRK2, and G $\alpha$ q/11. *J Biol Chem.* 2011;286:19259-19269. doi:10.1074/jbc.M111.239772
34. Subramanian H, Gupta K, Parameswaran N, Ali H. Regulation of Fc $\epsilon$ R1 signaling in mast cells by G protein-coupled receptor kinase 2 and its RH domain. *J Biol Chem.* 2014;289:20917-20927. doi:10.1074/jbc.M113.523969
35. Wang Y, Lee Y, Zhang J, Young KH. Identification of peptides that inhibit regulator of G protein signaling 4 function. *Pharmacology.* 2008;82:97-104. doi:10.1159/000138387
36. Lerner TN, Kreitzer AC. RGS4 is required for dopaminergic control of striatal LTD and susceptibility to parkinsonian motor deficits. *Neuron.* 2012;73:347-359. doi:10.1016/j.neuron.2011.11.015
37. Turner EM, Blazer LL, Neubig RR, Husbands SM. Small molecule inhibitors of regulators of G protein signaling (RGS) proteins. *ACS Med Chem Lett.* 2012;3:146-150. doi:10.1021/ml200263y
38. Blazer LL, Roman DL, Chung A, et al. Reversible, allosteric small-molecule inhibitors of regulator of G protein signaling proteins. *Mol Pharmacol.* 2010;78:524-533. doi:10.1124/mol.110.065128
39. Noor F, Niklas J, Müller-Vieira U, Heinzle E. An integrated approach to improved toxicity prediction for the safety assessment during preclinical drug development using Hep G2 cells. *Toxicol Appl Pharmacol.* 2009;237:221-231. doi:10.1016/j.taap.2009.03.011
40. Arnott JA, Planey SL. The influence of lipophilicity in drug discovery and design. *Expert Opin Drug Discov.* 2012;7:863-875. doi:10.1517/17460441.2012.714363
41. Tesmer JGG, Berman DM, Gilman AG, Sprang SR. Structure of RGS4 Bound to AIF4 $\Delta$ -Activated G $\alpha$ i1: stabilization of the Transition State for GTP Hydrolysis, (n.d.) 11.
42. Sterne-Marr R, Dhami GK, Tesmer JGG, Ferguson SSG. Characterization of GRK2 RH domain-dependent regulation of GPCR coupling to heterotrimeric G proteins. In *Methods Enzymol.* Elsevier. 2004;310-336. doi:10.1016/S0076-6879(04)90020-1
43. Dahlin JL, Inglese J, Walters MA. Mitigating risk in academic pre-clinical drug discovery. *Nat Rev Drug Discov.* 2015;14:279-294. doi:10.1038/nrd4578

**How to cite this article:** Echeverría E, Ripoll S, Fabián L, Shayo C, Monczor F, Fernández NC. Novel inhibitors of phosphorylation independent activity of GRK2 modulate cAMP signaling. *Pharmacol Res Perspect.* 2022;10:e00913. doi:[10.1002/prp2.913](https://doi.org/10.1002/prp2.913)